



Improvement of Directed Energy Deposition (DED) material addition rate via fluence-based parameter scaling method

Kyle Odum¹ · Leslie Leung¹ · Masakazu Soshi¹ · Kazuo Yamazaki²

Received: 11 January 2021 / Accepted: 13 September 2021 / Published online: 28 September 2021
© The Author(s), under exclusive licence to Springer Nature Switzerland AG 2021

Abstract

Directed Energy Deposition (DED) is a metal additive manufacturing process where feedstock (metal powder in this study) is delivered to a melt pool on the surface of a metallic part simultaneously with an energy source (a laser in this study) that causes the local melting. DED process productivity is measured using the Material Addition Rate (MAR) which is a measure of the amount of material that is added to the part per interval of time, while process efficiency is measured with the powder catchment efficiency which is the ratio of powder deposited into the part and powder fed through the nozzle during the deposition cycle. If clad geometry can be maintained while deposition head feed rate is increased, then MAR is increased. As DED functionality has been integrated into industrial CNC machining centers published deposition head feed rates in literature have not kept up with machine feed rate capabilities. This research demonstrates a method of using energy and powder fluence into the melt pool to scale up deposition head feed rate in a DED equipped CNC machining center to improve MAR while maintaining part quality and geometric accuracy.

Keywords Directed Energy Deposition · Additive manufacturing · Productivity · Porosity · Tensile testing

1 Introduction

Directed Energy Deposition (DED) is an additive manufacturing technology that uses a concentrated energy source to locally melt the surface of a metallic part creating a melt pool, into which a feedstock is deposited. The feedstock melts on contact and is incorporated into the melt pool. Upon cooling, the molten material in the melt pool solidifies fusing the feedstock to the substrate in a clad track [1]. Desired part geometry is built up by depositing subsequent clad tracks. This study focuses on the use of a high-power laser as the energy source and pneumatically conveyed metal powder as the feedstock.

Productivity of DED is measured by the material addition rate (MAR), which is the speed that material is deposited into the part (reported in mass or volumetric terms). Volumetric MAR is the product of clad cross section, a_{clad} , and deposition head feed rate, f :

$$\text{MAR} \equiv \frac{dV_{\text{part}}}{dt_{\text{cycle}}} = a_{\text{clad}} \cdot f. \quad (1)$$

The appearance on the market of DED and hybrid machine tools based on modified machining centers has raised the possibility of high productivity DED in industry. However, a brief, non-exhaustive survey of literature regarding DED research shows that, in general, feed rates reported in the DED literature have not kept pace with increased machine capability as much of the DED research pursued in academia is done on smaller, less powerful machines, Fig. 1.

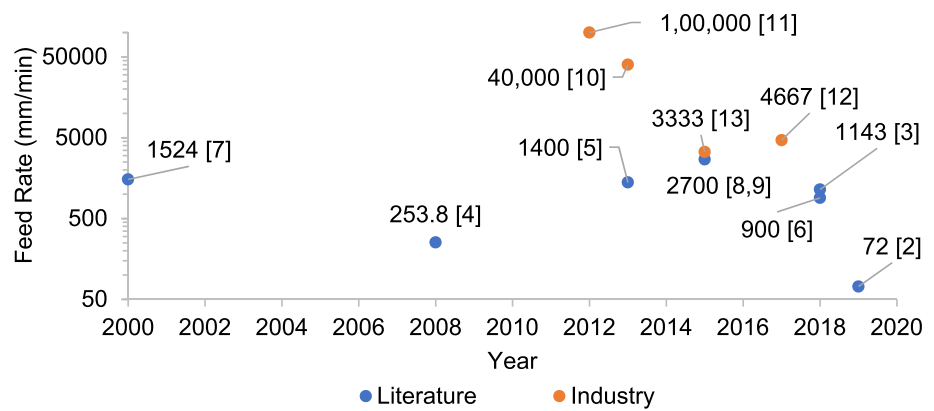
Like feed rate capabilities, laser power and powder flow rate capabilities of modern DED machines on the market have increased over time. As per Eq. (1), MAR can be increased if the clad cross section geometry is maintained while the deposition head feed rate is increased. Process windows for DED reported in literature have indicated that with sufficient laser power, laser spot size, and powder flow

✉ Masakazu Soshi
msoshi@ucdavis.edu

¹ Advanced Research for Manufacturing Systems (ARMS) Laboratory, Department of Mechanical and Aerospace Engineering, University of California, Davis, Davis, CA, USA

² IMS-Mechatronics Laboratory, Department of Mechanical and Aerospace Engineering, University of California, Davis, Davis, CA, USA

Fig. 1 Comparison of maximum feed rates in literature and in industrial DED machine tools with respect to year of publication or product release



rate into the melt pool, the feed rate of the deposition head can be increased without excessive clad porosity or dilution [14], though changes in microstructure [15] and phase [16] of the deposited material can be affected by energy fluence.

Full utilization of the dynamic capabilities of modern DED equipped machine tools requires a method for extending DED process parameters to higher deposition head feed rates. While it has been shown that alternative toolpaths can be used to increase MAR [17], not all part features are amenable to nonlinear toolpaths. This research proposes using an energy and mass fluence-based methodology, similar to the heat input per unit length used in welding [18], for modification of DED process parameters to increase MAR with higher deposition head feed rates using linear toolpaths. Research has shown that manipulation of fluence values can be used to control clad geometry of thin wall DED parts [19] by managing the heat accumulation identified by [20]. Extrapolating clad geometry dependencies on energy and mass fluence values determined from simple, single line DED experiments laser power, powder mass flow rate, and deposition head feed rate were modified for a simple thin wall part. Mechanical properties and porosity of the more productively deposited DED thin wall parts was compared to thin walls deposited with more conservative, industry and literature standard DED parameters. In addition to thin wall deposition experiments, a large part was deposited with the high productivity DED parameters using positional and simultaneous 5-axis machine motion to demonstrate the applicability of the fluence-based technique to larger, more complex parts.

2 Theory and calculation

2.1 DED parameter fluence values

Borrowing the method of using heat input per unit length from welding literature [18], the energy fluence, EF, of the laser into the melt pool is calculated as the ratio of laser

power, P , and the product of laser spot diameter, d , and deposition head feed rate, f :

$$EF = \frac{P}{d \cdot f} \quad (2)$$

Similarly, a powder mass flow fluence, PF, is calculated as the ratio of the powder mass flow rate through the deposition head, \dot{m} , and the product of the laser spot diameter and deposition head feed rate:

$$PF = \frac{\dot{m}}{d \cdot f} \quad (3)$$

EF has SI units of $\frac{J}{m^2}$ and PF has units of $\frac{kg}{m^2}$. The laser optics in the equipment used in this study were fixed and the working distance of the deposition head to the substrate was also kept constant so the laser diameter was static at approximately 3 mm. Balancing EF and PF was done via manipulation of laser power, powder mass flow rate, and deposition head feed rate only.

3 Methods

3.1 DED equipment and deposition experiments

A DMG Mori (Nagoya, Japan) LaserTec 65 3D Hybrid (hybrid machine) A-C 5-axis machining center was used for DED experiments in this study. The hybrid machine was equipped 2.5 kW Laser Line (Mülheim-Kärlich, Germany) 1020 nm diode laser module connected to a deposition head fitted with a Fraunhofer (Munich, Germany) COAX9 coaxial deposition nozzle via an optical fiber. Powder is supplied from a GTV (Luckenbach, Germany) PF 2/2 disk-hopper type powder feeder. The spindle of the hybrid machine is capable of linear feed rates of 40 m/min in the X , Y , and Z axes, although linear feed movements are limited when the deposition head is in the spindle to 5000 mm/min to protect the optical fiber. All DED process parameters were

controlled from the Siemens (Munich, Germany) 840D controller on the hybrid machine.

The powder feedstock used in DED experiments was Oerlikon (Pfäffikon, Switzerland) MetoClad 316L stainless steel gas atomized powder with a size range of 54–104 μm. Powder was deposited from sealed containers sent by the supplier directly into the powder hopper in the machine. Prior to DED experiments, the powder mass flow rate through the nozzle was determined with a 2-min powder flow test repeated 3 times to ensure an accurate powder delivery rate. Both shielding and carrier gas used during DED experiments was 99.999% ultra-high purity argon. Substrates used in DED experiments were unfinished 101.5 mm × 101.5 mm × 25.4 mm blocks sectioned from a piece of hot rolled, annealed 316L stainless steel bar stock. Substrates were held in a Kurt (Minneapolis, MN, USA) vise bolted to the hybrid machine table.

Experimental investigation of clad geometry relations to EF and PF consisted of:

1. An initial design of experiments (DOE) of single line clads over a range of DED parameter values.
2. Modification of DED parameters based on EF and PF relationships with clad geometry to increase MAR.
3. Deposition of thin wall DED parts with high MAR parameters followed by an analysis of part porosity and tensile strength.
4. Demonstration of cycle time savings from use of high MAR DED parameters during deposition of a large, flared cylindrical case study part.

Initial DED experiments consisted of a full-factorial design of experiments (DOE) for 153 90 mm long single line clads using the linear axis feed rates, powder mass flow rates (PFR), and laser powers in Table 1.

DOE values were selected to lie between the industry standard values and the machine maximum capability for each of the factors except powder mass flow rate. A wider range of powder mass flow rate was investigated to ensure that any increases in MAR due to an increased powder catchment efficiency at high feed rates with high laser power and low powder mass flow could be observed.

Additionally, the base case of 1000 mm/min feed rate, 13.5 g/min PFR, and 1800 W laser power (following

guidance from the DED machine tool manufacturer which also falls within the general range of values used in DED literature) was tested for comparison. Up to 9 single line clads were deposited onto a substrate spaced 10 mm apart with 20 s between single line depositions.

After the initial single line clad DOE, 2 sets of DED parameters were derived that were expected increase MAR while maintaining part material quality and geometric accuracy. Enhanced MAR parameter sets and more conservative machine manufacturer recommended DED parameters typical of those reported in the literature were used to deposit 90 mm long by 90 mm tall by 4.6 mm wide thin wall parts with 2 passes per layer using both raster and bidirectional toolpaths, Fig. 2.

All thin wall toolpaths included a 3-s inter-pass dwell to allow for meltpool heat to diffuse into the part. Thin wall depositions were done one at a time on substrates with the same dimensions and composition as the single line tests. After cooling to room temperature under free convection in the deposition chamber of the hybrid machine the thin walls were cut from the substrate using a Marvel (Oshkosh, WI, USA) vertical bandsaw with coolant. After removal of the thin wall, the substrate was allowed to dry in ambient air and the next thin wall was deposited on the substrate 10 mm from the previous one similar to the single line clads.

The flared cylindrical case study part was deposited onto a cylindrical mild steel substrate 140 mm in diameter and 9.5 mm thick that was fixtured in a three-jaw chuck on the table of the hybrid machine. During deposition of the cylindrical test part, the linear feed motions were programmed to mainly be achieved via C-axis table rotation. Using simultaneous 5-axis control, the Y-axis and Z-axis spindle movement was executed along with an A-axis table tilt to build

Table 1 Parameter levels for full-factorial design matrix of single line clad DED experiments

Factor	Levels
Feed rate (m/min)	2, 3, 4, 5
Powder mass flow rate (g/min)	10, 14, 18, 22, 26, 30
Laser power (kW)	1.9, 2.1, 2.3, 2.5

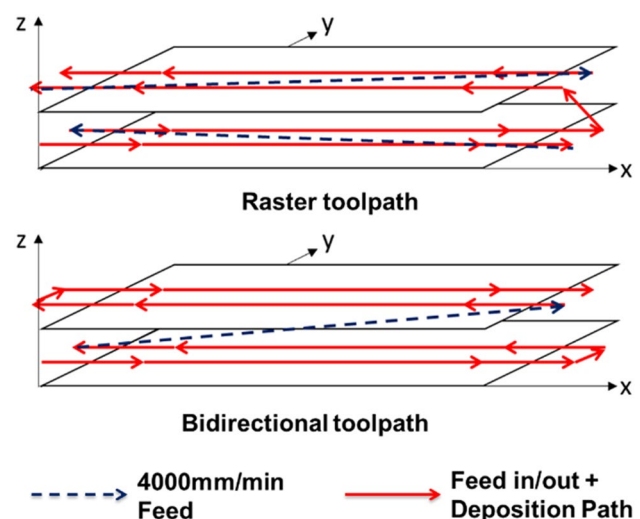


Fig. 2 Two-layer depiction of the raster toolpath (top) and the bidirectional toolpath (bottom)

the test part. The test part was deposited in 3 program cycles with sufficient cooling time between depositions for the part to cool to room temperature under free convection while in the work holding chuck on the machine table.

3.2 Metrology equipment and data processing

Single line clad geometry height measurements were collected using a MicoEpsilon (Ortenburg, Germany) LSM2 dispersive laser measurement unit mounted in a MicroVu (Windsor, CA, USA) Excel 502HC, Fig. 3a. Height measurements were taken at a sampling pitch of 0.05 mm in the direction normal to the major clad axis and 0.5 mm in the direction parallel to major clad axis, Fig. 3a. All scan segments were combined into a single representative cross section using a mean bin average of 0.05 mm wide bins. Edges of the clad were determined from inflection points in bin averaged clad data after median filtering with a 15-bin window. A second-order polynomial centered at the maximum bin averaged value of the data was calculated using a least

square fit, Fig. 3b. Clad heights were computed as the zero-order polynomial term and clad widths were computed as the difference of the polynomial roots.

Micrographs of deposited thin walls were collected using a Hitachi (Tokyo, Japan) TM-1000 scanning electron microscope (SEM). SEM samples were prepared by mounting sectioned DED thin wall samples into Buehler (Lake Bluff, IL, USA) Conductomet graphite powder using a Buehler SimpliMet 1000 mount press, which were then polished on a Buehler Ecomet 3 polishing station. SEM images were collected at 1200 times magnification from three different locations on each sample. A script was written to extract pore information from the SEM images using the following method:

1. Raw grayscale images, Fig. 4a, were binarized based on a global threshold value, Fig. 4b.
2. A disc-shaped morphological structuring element was used to define the pores and remove the polishing striations from the binarized images, Fig. 4c.

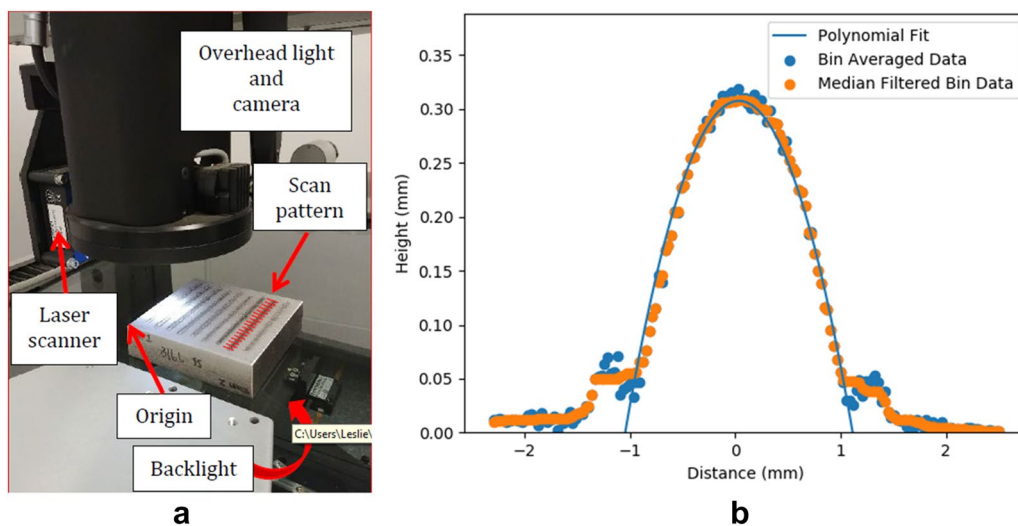


Fig. 3 a MicroVu scanning setup and b polynomial fit of bin averaged clad height data

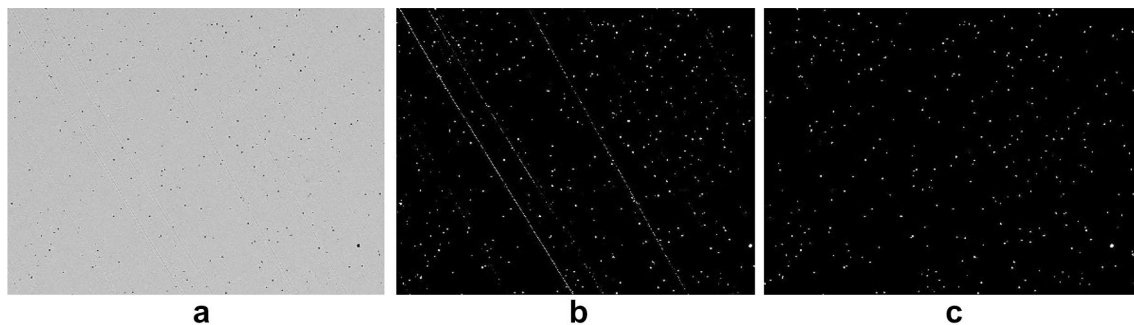


Fig. 4 a SEM image of DED thin wall, b binarized SEM image, and c filtered SEM image using disk shaped structuring element

- Pore fraction was computed as a ratio of the total combined pixel area of the structural elements to the total pixel area of the SEM image.

Tensile test specimens were machined from the DED thin walls for testing on an Instron (Norwood, MA, USA) 33R4204. Using a strain rate of 2.54 mm/min and an initial post-calibration load of 50 N, the samples were tested until failure or a strain of 0.42 due to the thickness of the samples. Three samples were prepared from both parallel and perpendicular to the build direction, Fig. 5. A tensile specimen was also machined from wrought stainless steel for comparison to the DED samples.

4 Results and discussion

The main effects plots of the single line DOE indicate a strong, clear direct correlation between powder flow and clad height, a weak, noisy inverse correlation between feed rate and clad geometry, and a less clear direct correlation between laser power and clad width, Fig. 6.

When feed rate is incorporated into the most significant factors for clad height and width using the fluence formulae from (2) and (3), the direct correlation of the main effects of EF on clad width and PF on clad height are very clear, Fig. 7.

Based on the main effects from the single line DOE, data regression analysis was used to create simple models for the relationships between EF and clad width, as well as, PF and clad height. EF values to clad width was found to follow an exponential regression model for clad, Fig. 8:

$$w = 3.31 * [1 - \exp(-1.11 * EF)] \tag{4}$$

The exponential regression model (4) is asymptotic to 3.31 mm at EF values within the process window for DED. This is logical as the laser spot diameter is roughly 3 mm. Depositing a clad much wider than the laser spot requires very large energy fluence values either from excessively high laser power or slow deposition head feed rates. Both conditions lead to poor deposition due to excessive dilution [14], powder diversion from the melt pool due to plasma plume eruptions [21], and excessive porosity in the deposited material [22]. Additionally, the EF value must be maintained at a level that supports full feedstock melting to avoid lack of fusion defects and poor powder catchment efficiency [23].

A linear relationship between clad height, *h*, and PF was observed from single line DOE data consistent with literature [24], Fig. 9.

The linear model for clad height was found to be:

$$h = 1.532 * PF \tag{5}$$

If EF and PF values are maintained from the base line DED parameter set, the maximum feed rate possible in the

Fig. 5 Schematic of tensile test samples **a** parallel to the build direction, **b** perpendicular to the build, **c** drawing of tensile test specimen dimensions, and **d** machined tensile specimens in fixture

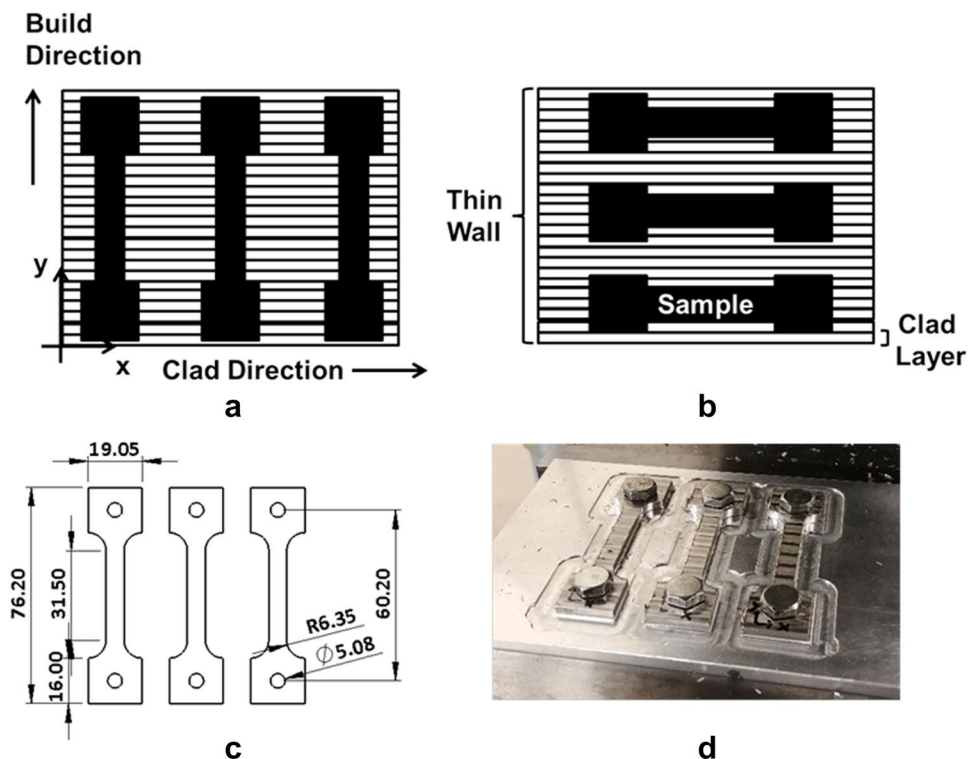


Fig. 6 Main effects of single line clad DOE with trends in mean clad widths (top row) and mean clad height (bottom row)

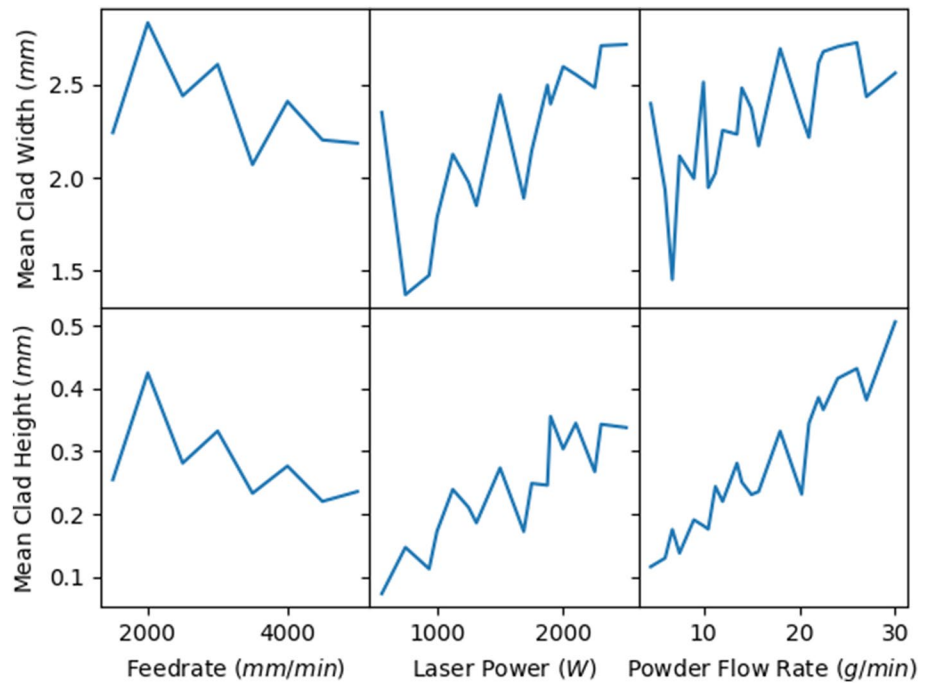


Fig. 7 Main effects of EF on clad width and PF on clad height

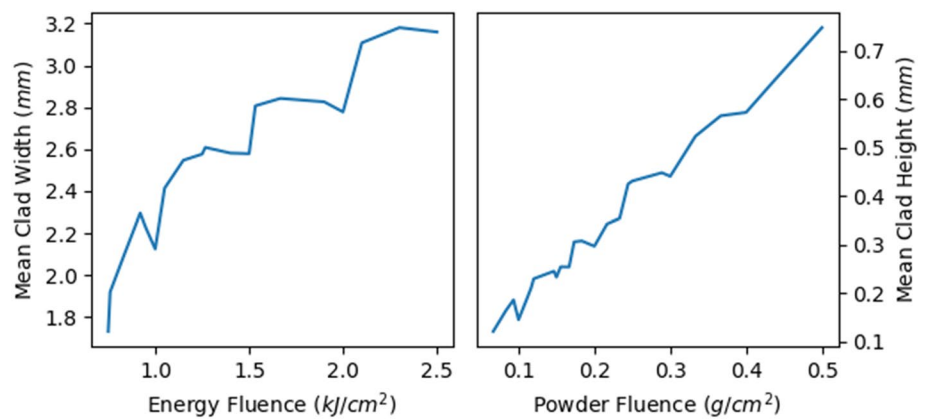


Fig. 8 a Exponential regression for clad width and energy flux with 95% confidence interval as dashed line and **b** accuracy of clad width model with 95% confidence interval as dashed line

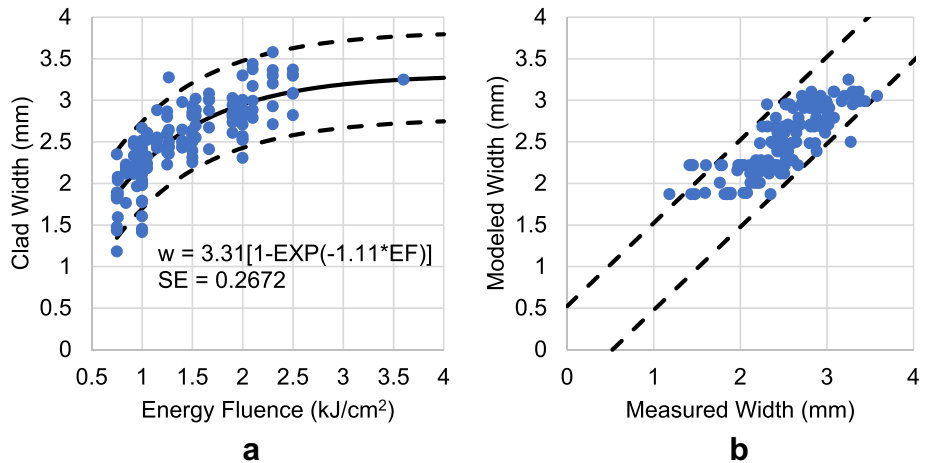
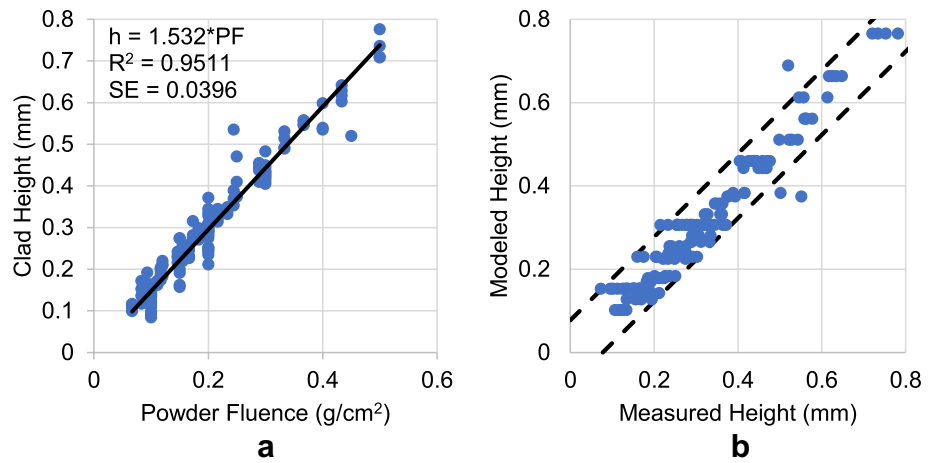


Fig. 9 **a** Linear regression for clad height and powder flux with 95% confidence interval as dashed line and **b** accuracy of clad height model with 95% confidence interval as dashed line



hybrid machine is limited by the maximum laser power of the machine. However, during deposition of tall DED parts with many layers, it is common to reduce the laser power as the DED cycle progresses while maintaining feed rate due to heat accumulation within the part [24]. The reduction of laser power is on the order of 25% of the initial laser power per the machine manufacturer. Due to the asymptotic relationship between EF and clad width, a 25% reduction in EF yields a clad that is only 3% narrower than the base line case.

Based on the recommended 25% EF reduction for longer builds EF values of $3.0 \frac{\text{kJ}}{\text{cm}^2}$ and $2.78 \frac{\text{kJ}}{\text{cm}^2}$ were used for high MAR parameter development (EF reductions of 17% and 23%, respectively). Feed rates were determined from (2) with the laser power set to the machine maximum of 2.5 kW. The powder flow rate for high MAR parameter set 1 was set using (3) to match the base line DED parameter set. Powder flow rate for high MAR parameter set 2 was chosen as $30 \frac{\text{g}}{\text{min}}$ to test near the machine maximum of the hybrid machine. The capabilities of the hybrid machine used in experiments, the machine manufacturer recommended base line parameter set, and the two high MAR DED parameter sets used in testing are listed in Table 2.

High MAR parameter sets were tested in single line experiments to check the validity of the clad geometry regression models. Clad height was overestimated by the regression model with the base case error at 32.6%, set 1

error at 9.4%, and set 2 error at 10.5% above the measured height. Clad width was more accurately modeled with width prediction errors of 2.5% for the baseline set, -2.4% for set 1, and -0.4% for set 2, Fig. 10.

MAR was increased in the single line tests by > 110% and powder efficiency, the ratio of rate of change for clad mass to powder mass flow rate through the nozzle, by > 12% as compared to the base line DED parameter set, Table 3.

Thin wall builds were executed using both the base line and high MAR parameter sets with the interlayer deposition head retract height set to the measured height values from single line testing. Tensile testing and SEM samples were prepared from thin wall builds. Porosity was observed to be inversely proportional to MAR in the thin wall tests, Fig. 11. As the energy and mass fluence were balanced while increasing feed rate, the increase in porosity at high feed rates that has been reported due to lack of fusion defects [25] was not observed.

Mean pore diameter was also observed to be inversely proportional to MAR, Fig. 12.

The ultimate tensile strength of DED samples was anisotropic with differences of > 2.5% observed between loading directions in all samples, Fig. 13. This is consistent with literature and is due to comparatively weaker bonds between layers due to defects such as pores [26] and the orientation of the grains and dendrites along the build direction in DED

Table 2 DED Parameter sets used in thin wall testing (*estimated)

Parameter	Feed rate (mm/min)	Laser power (kW)	Powder flow rate (g/min)	EF (kJ/cm ²)	PF (g/cm ²)	Clad width (mm)	Clad height (mm)
Hybrid machine maximum	5000	2.5	> 30	–	–	–	–
Base line parameter set	1000	1.8	13.5	3.6	0.45	3.25	0.52
High MAR Set 1	1666	2.5	22.5	3.0	0.45	3.19*	0.69*
High MAR Set 2	1800	2.5	30	2.78	0.56	3.16*	0.85*

Fig. 10 Actual vs predicted clad geometry from MAR optimized single line clads

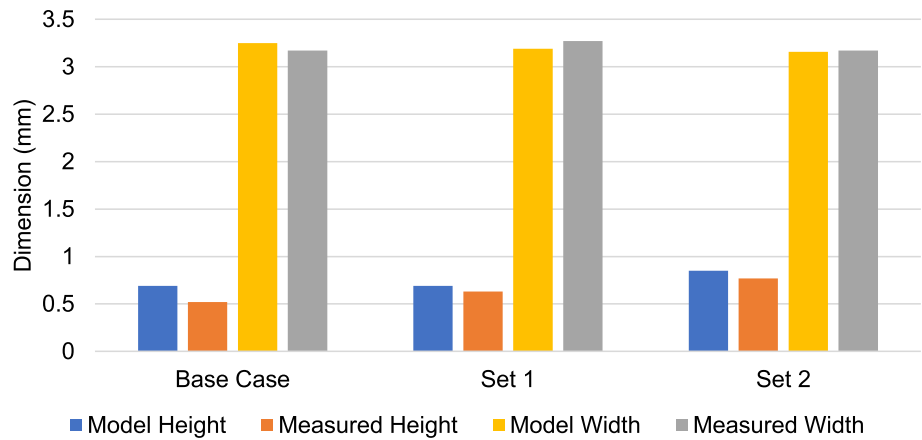


Table 3 Clad geometry and MAR from thin wall DED tests

Parameter	Feed rate (mm/min)	Clad width (mm)	Clad height (mm)	MAR (cm ³ /h)	Powder efficiency (%)
Base line Set	1000	3.17	0.52	70.2	69
High MAR Set 1	1667	3.27	0.63	147.6	87
High MAR Set 2	1800	3.17	0.77	184.2	81

parts that help facilitate dislocation propagation through the material [27].

The horizontal ultimate stress (in the direction of laser travel) was seen to decrease with increasing MAR, though the vertical ultimate stress (in the direction normal to the layers) was seen to initially decrease with increasing MAR then drastically increase at the highest MAR to values near the wrought sample. A similar trend was observed in the

yield stress though the increase at the highest MAR was less dramatic and was also observed in the horizontal loading direction. No clear trend was observed in the elongation at failure data. All strength data exhibited a large standard deviation typical of DED material, Fig. 13.

To extend the findings of the thin wall experiments a large, cylindrical part with a top flare was deposited with the high MAR parameter set 1. Set 1 was chosen due to the superior powder efficiency as compared to set 2, while still exhibiting an MAR value more than twice the machine manufacturer’s recommended parameters.

The test part was a 117.6 mm tall and was deposited in 3 operations, color coded in Fig. 14. All sections of the test part were deposited in a continuous single pass. Deposition was carried out using both positional and synchronous 5-axis machine motions. Cycle time was recorded directly from the controller for comparison to dry runs of demonstration part operation codes from the machine manufacturer.

A comparison of cycle time from the optimized DED parameters to the baseline parameters shows a reduction of 61% in cycle time, Fig. 15.

Fig. 11 Mean area porosity versus MAR

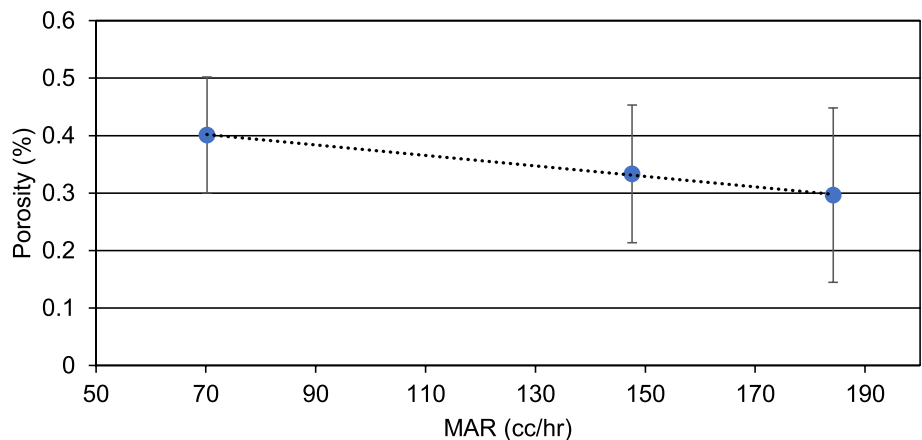


Fig. 12 Mean pore diameter versus MAR

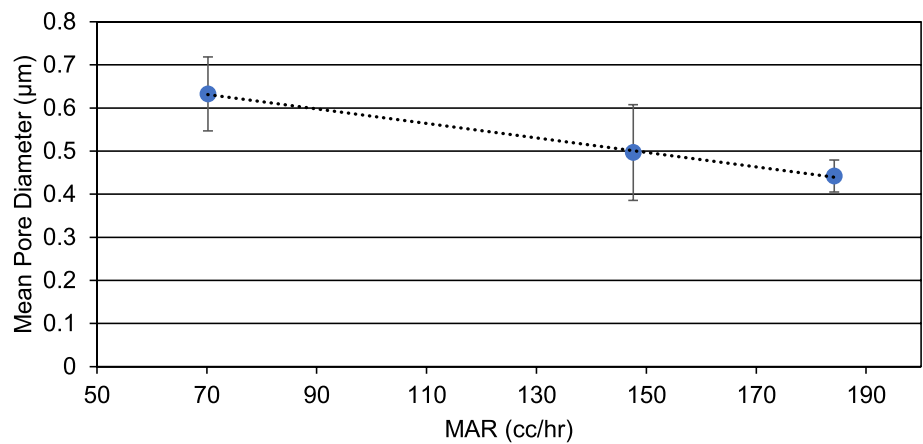
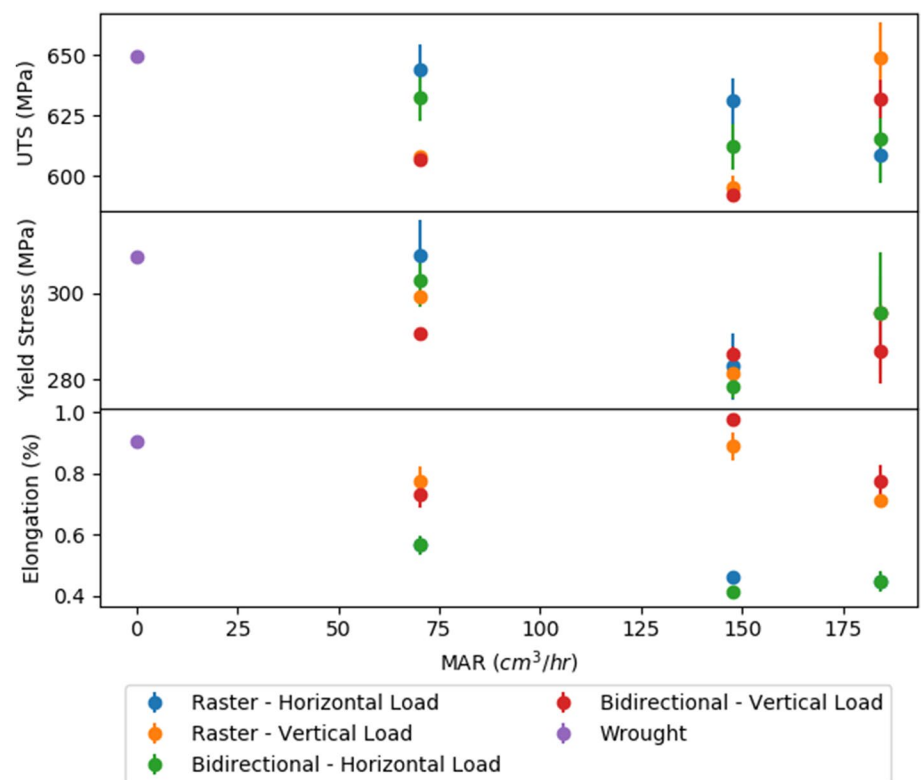


Fig. 13 Tensile testing results versus MAR from thin wall samples with ultimate tensile strength (top), yield strength (middle), and elongation at failure (bottom)



5 Conclusion

Currently there is an imbalance between the capabilities of DED equipped machine tools on the market and the reported deposition parameter settings in much of the published literature regarding DED, with many published studies using slow deposition head feed rates and low laser powers and powder mass flow rates. Increasing deposition head feed rate is a means to increase the MAR of a DED operation if the clad geometry is to be maintained. The relationship between laser and powder fluence values into the melt pool and clad geometry was modeled based on the

output of a full-factorial DOE of single line DED clads. Fluence–geometry relationships observed in the single line DOE data were used to scale DED parameters to increased MAR by increasing deposition head feed rate. Mechanical properties and porosity of thin wall parts deposited using high MAR parameter sets were compared to thin walls deposited using a more conservative, literature and industry standard DED parameter set that yields a lower MAR. The results of the thin wall tests with high MAR DED parameters were:

- Porosity was seen to decrease with increasing MAR.

Fig. 14 **a** Test part solid model with operations color coded, **b** Cross section drawing with dimensions, **c** substrate in chuck, **d** end of operation 1, **e** end of operation 2, and **f** end of operation 3

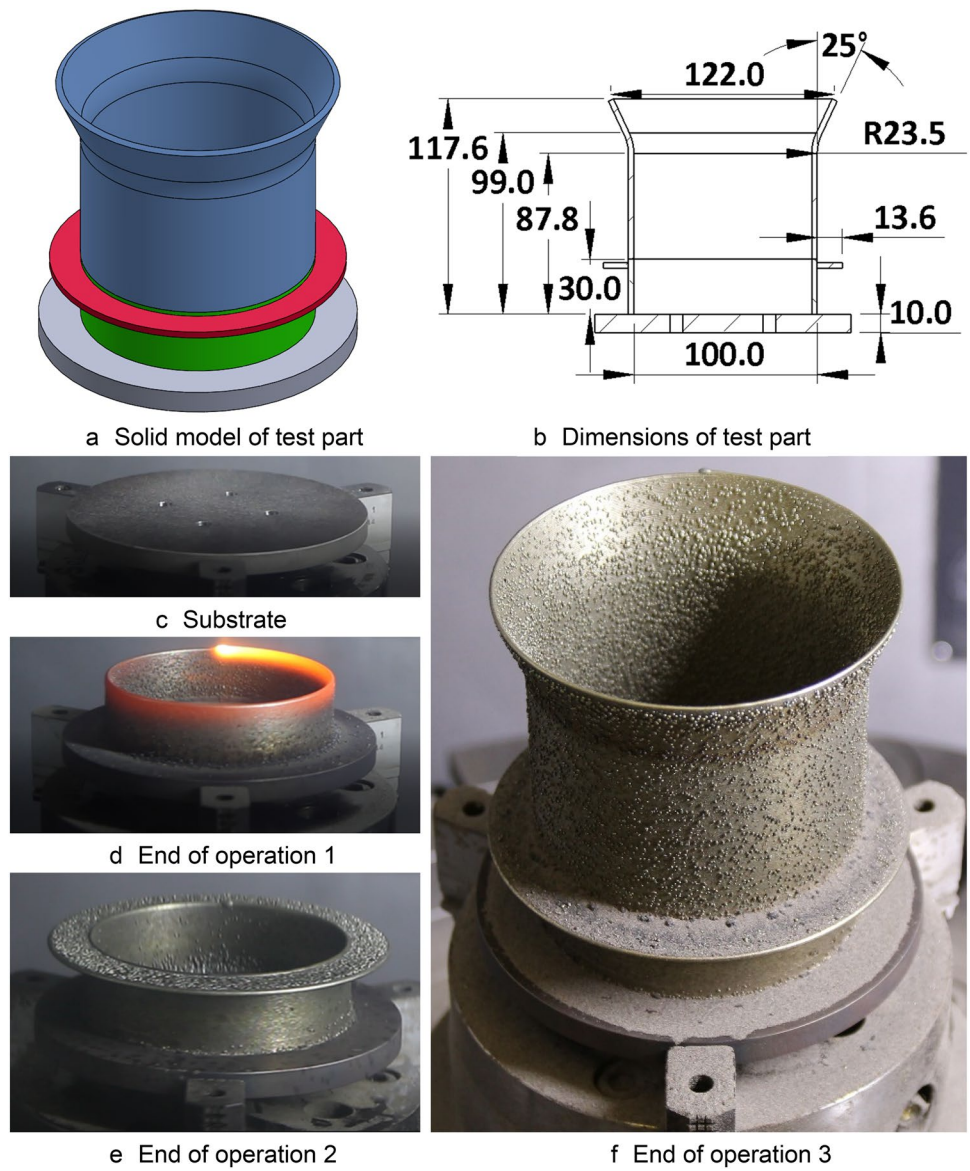
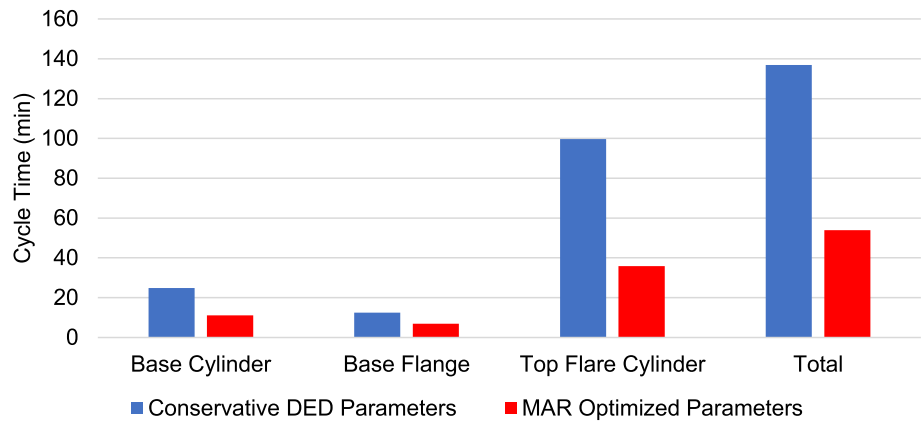


Fig. 15 Cycle time comparison for conservative and MAR optimized DED parameters



- No clear trends were observed in the ultimate tensile stress, yield stress, and elongation at failure as a function of MAR.
- Powder efficiency was seen to increase in the high MAR thin wall deposition tests.

Using the most powder efficient of the high MAR DED parameter sets, a large, complex test part was deposited using simultaneous 5-axis machine motion to demonstrate the viability of high MAR DED parameters for industrial use. High MAR DED parameters produced the test part 61% faster than more conservative DED parameters.

Funding This research did not receive any specific grant from funding agencies in the public, commercial, or not-for-profit sectors.

Declarations

Conflict of interest On behalf of all authors, the corresponding author states that there is no conflict of interest.

Data availability Not applicable.

Code availability Not applicable.

References

1. ASTM International. 2016. ASTM F3187–16: standard guide for directed energy deposition of metals, USA
2. Rashkovets M, Nikulina A, Klimova-Korsmik O (2019) High-speed direct laser deposition of 51Ni-14Co-10Cr-6Al-5Mo alloy: microstructure and phase composition. *Mater Today Proc* 11:144–149
3. Sciammarella F, Salehi Najafabadi B (2018) Processing parameter DOE for 316L using directed energy deposition. *J Manuf Mater Process* 2(3):61
4. Tang L, Ruan J, Landers RG, Liou F (2008) Variable powder flow rate control in laser metal deposition processes. *J Manuf Sci Eng* 130(4):041016
5. Ma M, Wang Z, Wang D, Zeng X (2013) Control of shape and performance for direct laser fabrication of precision large-scale metal parts with 316L Stainless Steel. *Opt Laser Technol* 45(1):209–216
6. Fearon E, Watkins KG (2018) Optimisation of layer height control in direct laser deposition, no. 1708
7. Mazumder J, Debasish Dutta D, Kikuchi N, Ghosh A (2000) Closed loop direct metal deposition: art to part. *Opt Lasers Eng* 34(4–6):397–414
8. Turichin GA et al (2015) Technological aspects of high speed direct laser deposition based on heterophase powder metallurgy. *Phys Proced* 78:397–406
9. Turichin G, Zemlyakov E, Klimova O, Babkin K (2016) Hydrodynamic instability in high-speed direct laser deposition for additive manufacturing. *Phys Proced* 83:674–683
10. DMG Mori. 2021. LASERTEC 65 3D hybrid. [Online]. Available: <https://us.dmgmori.com/products/machines/additive-manufacturing/powder-nozzle/lasertec-65-3d-hybrid>.
11. Trumpf. 2021. TruLaser Cell 7040 [Online]. Available: https://www.trumpf.com/en_US/products/machines-systems/3d-laser-cutting/trulaser-cell-7040/.
12. BeAM. 2019. BeAM directed energy deposition
13. Hermle. 2019. Additive Manufacturing [Online]. Available: https://www.hermle.de/en/services/additive_manufacturing/technology_mpa/getPrm/entry/mpa_-_a_mpa_powder_application_technique/.
14. Steen WM, Mazumder J (2010) *Laser material processing*, 4th edn. Springer, London. <https://doi.org/10.1007/978-1-84996-062-5>
15. Joshi SS, Sharma S, Mazumder S, Pantawane MV, Dahotre NB (2021) Solidification and microstructure evolution in additively manufactured H13 steel via directed energy deposition: integrated experimental and computational approach. *J Manuf Process* 68:852–866
16. Zhang D, Li Y, Wang H, Cong W (2021) An investigation on Ni₄Ti₃ phase precipitation and its effects in laser directed energy deposition of TiC-NiTi composites. *Mater Sci Eng A* 809:140976
17. Soshi M, Odum K, Li G (2019) Investigation of novel trochoidal toolpath strategies for productive and efficient directed energy deposition processes. *CIRP Ann* 68(1):241–244
18. Oliveira JP, Santos TG, Miranda RM (2020) Revisiting fundamental welding concepts to improve additive manufacturing: from theory to practice. *Prog Mater Sci* 107:100590. <https://doi.org/10.1016/j.pmatsci.2019.100590>
19. Li G, Odum K, Yau C, Soshi M, Yamazaki K (2021) High productivity fluence based control of Directed Energy Deposition (DED) part geometry. *J Manuf Process* 65:407–417
20. Zhang Z, Liu Z, Wu D (2021) Prediction of melt pool temperature in directed energy deposition using machine learning. *Addit Manuf* 37:101692
21. Govekar E, Jeromen A, Kuznetsov A, Levy G, Fujishima M (2018) Study of an annular laser beam based axially-fed powder cladding process. *CIRP Ann* 67:241–244. <https://doi.org/10.1016/j.cirp.2018.04.082>
22. Debroy T, Wei HL, Zuback JS, Mukherjee T, Elmer JW, Milewski JO, Beese AM, Wilson-heid A, De A, Zhang W (2018) Additive manufacturing of metallic components—process, structure and properties. *Prog Mater Sci* 92:112–224
23. Dass A, Moridi A (2019) State of the art in directed energy deposition: from additive manufacturing to materials design. *Coatings* 9:418. <https://doi.org/10.3390/coatings9070418>
24. de Oliveira U, Ocelík V, De Hosson JTM (2005) Analysis of coaxial laser cladding processing conditions. *Surf Coat Technol* 197:127–136. <https://doi.org/10.1016/j.surfcoat.2004.06.029>
25. Hu Z, Zhu H, Zhang H, Zeng X (2017) Experimental investigation on selective laser melting of 17–4PH stainless steel. *Opt Laser Technol* 87:17–25. <https://doi.org/10.1016/j.optlastec.2016.07.012>
26. Ziętała M, Durejko T, Polański M, Kunce I, Płociński T, Zieliński W, Łazińska M, Stępniewski W, Czujko T, Kurzydłowski KJ, Bojar Z (2016) The microstructure, mechanical properties and corrosion resistance of 316 L stainless steel fabricated using laser engineered net shaping. *Mater Sci Eng A* 677:1–10. <https://doi.org/10.1016/j.msea.2016.09.028>
27. Yu J, Rombouts M, Maes G (2013) Cracking behavior and mechanical properties of austenitic stainless steel parts produced by laser metal deposition. *Mater Des* 45:228–235. <https://doi.org/10.1016/j.matdes.2012.08.078>